ELSEVIER

Journal of Power Sources 92 (2001) 250–254

JOURNAL OF POWER SOURCES

www.elsevier.com/locate/jpowsour

Hydrogen storage material based on $LaNi_5$ alloy produced by mechanical alloying

M.V. Simičić[a,*], M. Zdujić[b], D.M. Jelovac[a], P.M. Rakin[a]

[a]*Chemical Power Source Institute, Belgrade, Yugoslavia*
[b]*University of Belgrade, Institute of Technical Sciences-SASA, Belgrade, Yugoslavia*

Received 27 March 2000; received in revised form 26 June 2000; accepted 3 July 2000

Abstract

The electrochemical characteristics of the $La_{0.8}Ce_{0.2}Ni_{2.5}Co_{1.8}Mn_{0.4}Al_{0.3}$ compound, produced by mechanical alloying, are investigated for hydrogen storage in nickel-metal hydride (NiMH) batteries by discharging tests at constant current and by calculating equilibrium pressure of hydrogen from the equilibrium potentials. It is shown that the alloy produced by mechanical alloying, followed by annealing and activation exhibits high specific capacity at the stable potential plateau, even at the high discharge rate (10 mA cm^{-2}), and low hydrogen equilibrium pressure. The alloy of such composition gives low capacity loss during cycling, which enables its application for metal hydride battery production.

Keywords: Mechanical alloying; $LaNi_5$-based alloy; Hydrogen storage; Metal hydride electrode

1. Introduction

At the very beginning of $LaNi_5$ investigation, it was shown that capacity of hydrogenation considerably declines during cycling. After 100 charge–discharge cycles, capacity of hydrogenation dropped 40%, making the alloy inappropriate for battery application. Microscopic investigation showed that during cycling alloy particles become pulverised from starting dimension of 7 to 2 μm after 25 cycles [1]. This happened due to mechanical strain in crystal lattice, developed during charging process when volume expansion achieves 24%. Needle like crystals of $La(OH)_3$ were observed by Scanning Transmission Electron Microscopy (STEM). The decrease of the particle's size resulted in longer alloy surface exposure to electrolyte and increased alloy corrosion caused by high affinity of $LaNi_5$ to water according to the free energy changes associated with this reaction, −472 kJ (mol $LaNi_5$)$^{-1}$. During continuous pulverisation of $LaNi_5$ particles, La atoms were cast out to grain boundaries where $La(OH)_3$ is produced by oxygen corrosion of the alloy. Thus, the electrode surface is wetted by electrolyte solution and hydrogen storage capacity decreases.

Extensive research on hydrogen storage alloy was dealing with partial substitution of La and Ni by other elements, in order to reduce volume expansion ratio of alloy to its hydride [2]. Stability of the alloy is improved by a partial substitution of Co and Si for Ni and Nd for La [1]. It is shown that equilibrium pressure of the alloy decreases with the bringing in any of the following elements: Cr, Co, Cu, Al and Mn [3]. Cycle life was improved by the Ni substitution with the ternary solute in the order Mn<Cu<Cr<Al<Co. Another effect of these ternary substitutions for Ni, except Mn, was the increase of the overpotential for the desorption reaction. It is also shown that substitution of any of Ti [4], Zr [5], Nd [6] and Ce [7] atoms for La enhances the cycle lifetime. Unfortunately, the improvement of the number of cycles is accompanied with a decrease in the hydrogen absorption capacity, long activation or slow kinetics. Partial substitution of Sn for Ni has shown a 20-fold increase in the cycle lifetime over the binary alloy [8].

The research on alloys with partial replacement of Ni by definite amounts of Co showed that multicomponent alloys, based on $LaNi_{2.5}Co_{2.5}$, had much longer cycle life than others, though the replacement of Ni by Co brought about a considerable decrease in hydrogen storage capacity [1]. This significant improvement of cycle life, by substitution of Co for Ni, was associated with the reduction of volume expansion of crystal lattice during charging. It was observed that ternary alloy is more stable if a small amount of Si or Al, as for instance $LaNi_{2.5}Co_{2.4}Al_{0.1}$ or $LaNi_{2.5}Co_{2.4}Si_{0.1}$, is used as substitute for Co. These improvements were caused by forming protective surface layer around particles. The

* Corresponding author. Tel.: +381-11-3160772; fax: +381-11-194-991.
E-mail address: ihis@eunet.yu (M.V. Simičić).

0378-7753/01/$ – see front matter
PII: S0378-7753(00)00534-6

protective layer exists only if volume expansion of alloy is not too high. The mentioned effect can not be observed in binary $LaNi_5$ alloy. Zhang et al. [9] reported the use of Al atoms as a partial substituent for Ni. An accumulation of Al, as an insoluble oxide at the surface (possible mix metal oxide-alumina), serves as a protective film preventing long-term corrosion and extending the alloy's cycle life. The similar protective insoluble film formed by cerium oxide has been reported for Ce-containing alloy [10].

Mechanical alloying (MA) has been recently used to produce metal hydride materials [11,12]. The aim of this work was to investigate the electrochemical performance of the $La_{0.8}Ce_{0.2}Ni_{2.5}Co_{1.8}Mn_{0.4}Al_{0.3}$ alloy produced by MA process.

2. Experimental

Metal powders produced by Sigma-Aldrich Chemical Co. were used as starting material for mechanical alloying. They were: La (nominal purity of 99.9%, particle size 40 mesh), Ce (99.9%, 40 mesh), Ni (99%, 100 mesh), Co (99.9%, 100 mesh), Mn (>99%, 50 mesh) and Al (99%, 200 mesh). Powders were weighed to obtain the desired proportion of starting powder mixture of a total mass of 10 g. A stainless steel vial of an internal volume of approximately 220 cm^3, charged with 25 hardened-steel balls of diameter 8 mm was used as a milling medium. The ball-to-powder mass ratio was about 5. Prior to closing a vial, 1 ml of hexane as a process control agent was added to the powder mixture in order to reduce cold welding of powders. The vial was sealed with o-ring and the cover tightened by four screws.

All handling was done in a glove box filled with purified, dry (humidity $\leq$20 ppm) argon. Mechanical alloying was performed in a Fritsch Pulverisette planetary ball mill. The angular velocity of the supporting disk and vials was 33.2 (317 rpm) and 41.5 rad^{-1} (396 rpm), respectively. Milling was done for 27 h without any interruption. The impurity amount, 1.06 wt.% Fe and 0.14 wt.% Cr was determined by the inductively coupled plasma spectrometry (IPC). The powder closed into the quartz tube under purified argon atmosphere was annealed to temperature of 700°C for 48 h. The X-ray data (XRD) were collected at a Philips PW 1710 automatic diffractometer with Cu Kα graphite- monochromatized radiation (λ=0.1542 nm).

The powder was soaked in aqueous solution of KOH, of the density of 1.25 g cm^{-3} and treated at 70°C for one hour (activation treatment), rinsed and dried [13]. A mixture of 80% of activated powder, 15% graphite was homogenised in the mortar by pestle, followed by addition of 5% Teflon binder. The electrodes were fabricated by pressing the mixture onto an expanded Ni screen (35.4 MPa). The other electrode type had the same composition but the powder was not annealed and activated. The electrode cycling was carried out in open cell in 6 M aqueous solution of KOH with Hg/HgO (6 M KOH) reference electrode. A cut-off voltage of −0.500 V vs. reference electrode limited the time of discharge and charging was done to a charge return of 125%. Experiments were performed using an EGG 173 (PAR) galvanostat/potentiostat.

3. Results

Mechanical alloying consists of repeated fracture and cold welding of an elemental powder particles [14]. Mechanical alloying of the starting powder mixture, in argon atmosphere, produces very distorted structure (Fig. 1a). XRD analysis shows that powder consists of amorphous phase (wide diffused peak at $2\theta \approx 29°$) and traces of crystalline phase dispersed in amorphous matrix (smeared peak, close to nickel, at $2\theta \approx 44.5°$).

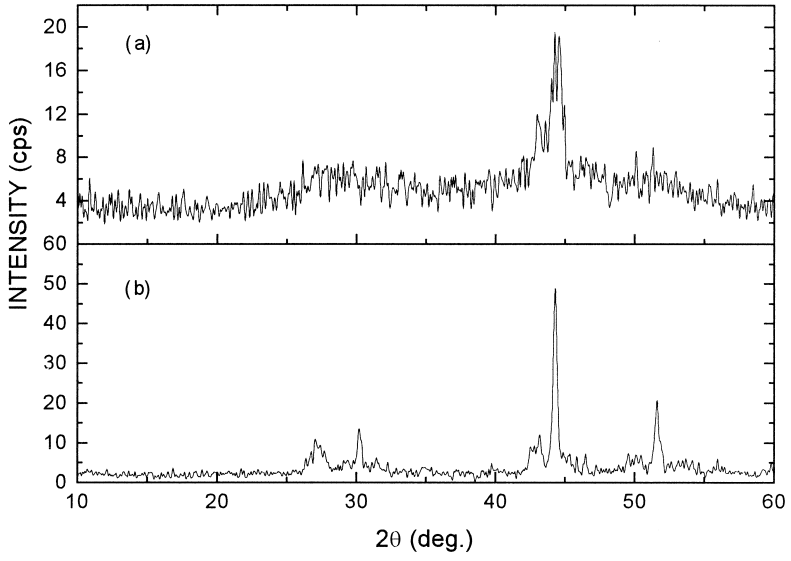

Fig. 1. XRD patterns of the $La_{0.8}Ce_{0.2}Ni_{2.5}Co_{1.8}Mn_{0.4}Al_{0.3}$ powder mixture after (a) mechanical alloying for 27 h and (b) subsequent heat treatment at 700°C for 48 h.

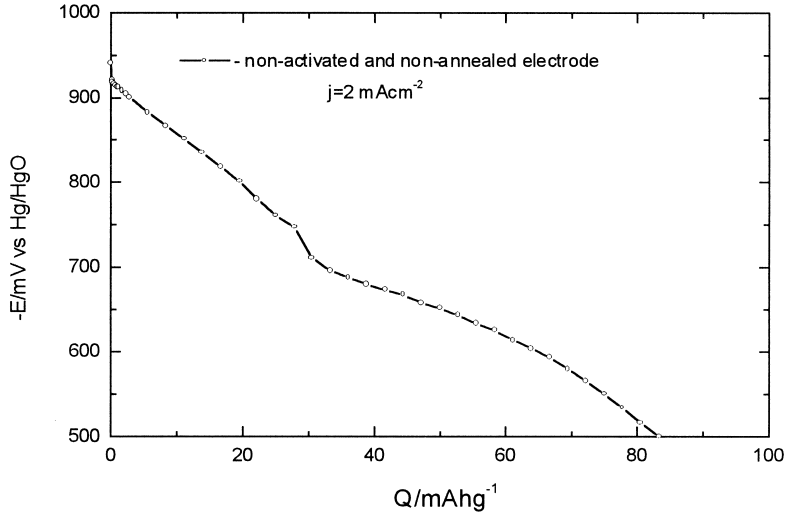

Fig. 2. Discharge curve of electrode fabricated with non activated and non-annealed powder.

The XRD pattern of annealed sample (Fig. 1b) is characterised by an appearance of well-crystallised lattice. Some of the peaks may be indexed on hexagonal unit cell of $CaCu_5$ type: peaks at $2\theta = 30.2$ and 43.2° ($d = 2.96$ and 2.09 Å, respectively), but not the others. The most intensive peaks at $2\theta = 48.9^\circ$ and 51.6° ($d = 2.04$ and 1.77 Å, respectively) may be assigned to Ni. However, they are systematically shifted to lower Bragg-angles indicating considerable increase of unit-cell volume. All these observations suggest that new intermetallic phase is produced by MA and annealing. Further studies are needed to characterise this phase.

Fig. 2 shows a typical discharge behaviour of the electrode, prepared from non activated and non-annealed powder. The electrode exhibited very poor characteristic, capacity lower than 90 mA h g^{-1} and two plateau caused by uncompleted diffusion inside the alloy particles.

Specific capacities of the electrode (activated and annealed alloy) during the formation period, are shown in (Fig. 3). The maximum electrochemical capacity was achieved in the fourth cycle and stayed constant over the period of 20 cycles. After 200 cycles electrode's capacity retention was greater than 85% of the capacity in the fourth cycle.

Fig. 4 shows typical discharging and charging curves with coulombic efficiency of 80% at $j = 2$ mA cm^{-2}. The potential of the hydride electrode in its equilibrium state, measured against a Hg/HgO reference electrode, corresponds to the pressure of the hydrogen gas on the surface, which is equilibrated with the atomic hydrogen in the hydride, according to the Nernst equation [5]. The hydrogen pressures calculated from the equilibrium potentials and the isotherms drawn from these data, are in a good agreement with the equilibrium hydrogen pressure obtained by conventional methods, based on a gas–solid reaction. Fig. 5 shows the electrochemical isotherm during desorption of hydrogen. It can be seen that the average equilibrium

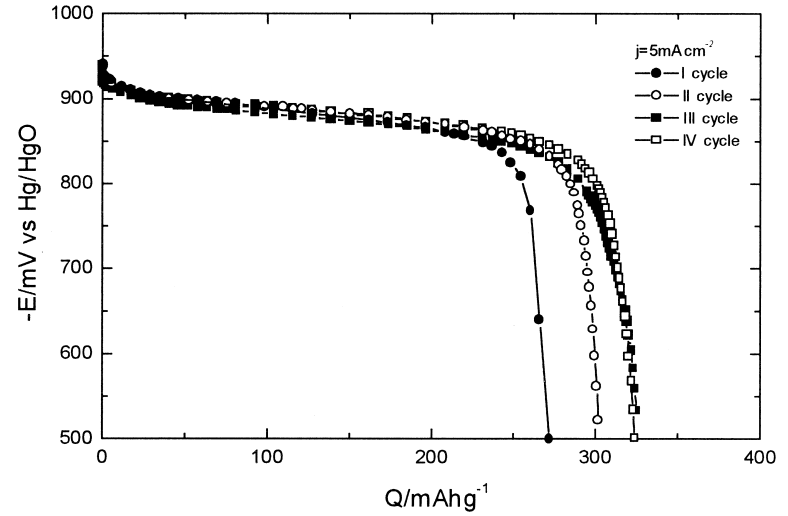

Fig. 3. Discharge curves during period of formation.

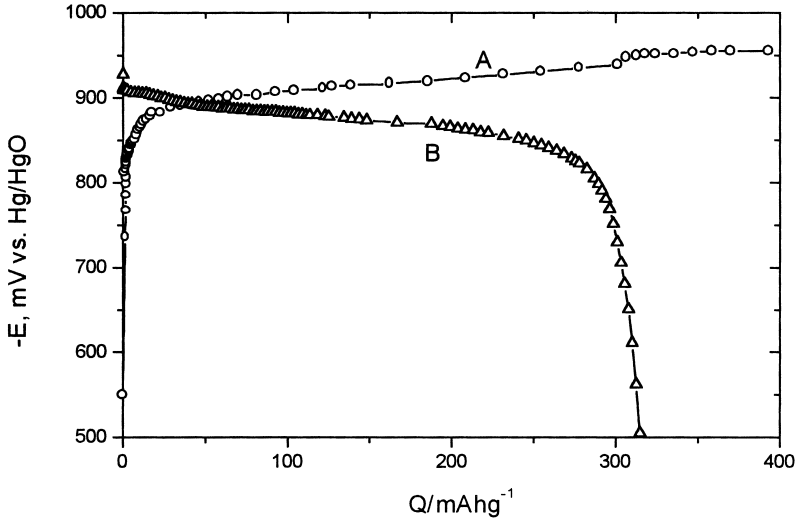

Fig. 4. Typical charge (A) and discharge (B) curves at $j = 5$ mA cm^{-2}.

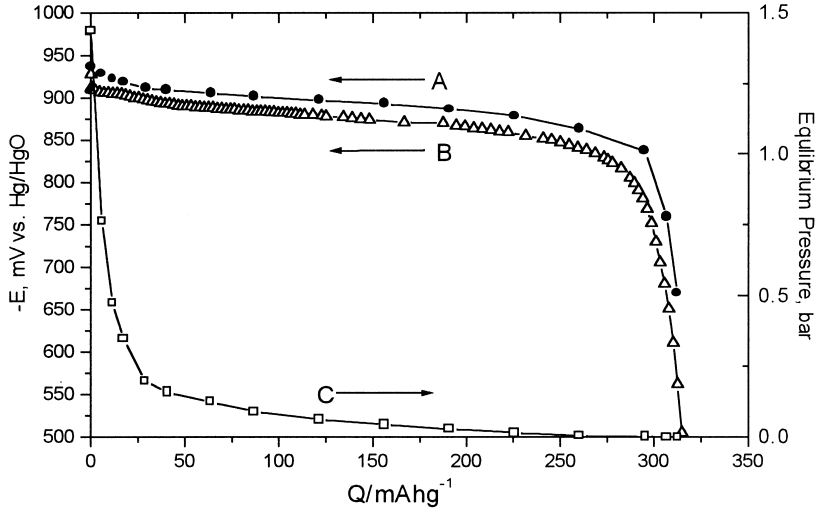

Fig. 5. Typical discharge curve (B), dependence of the equilibrium potentials (A) on capacity and calculated adsorption isotherm (C).

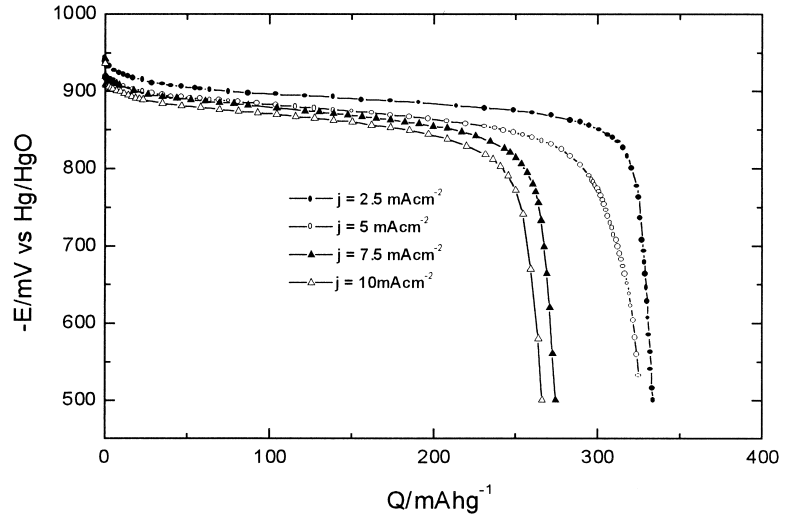

Fig. 6. Discharge curves as a function of discharge current densities.

plateau pressure of 0.035 bar is prominent compared with $LaNi_5$[5,15], $La_{0.9}Zr_{0.1}Ni_{4.5}Al_{0.5}$ [6], $LaNi_4Cu$ [15] and in the same order as $LaNi_4Al$ [15].

Fig. 6 shows discharging curves in the function of loads. It is evident that the behaviour of the electrode at $j = 10$ mA cm^{-2} (or 145 mA g^{-1}) is very satisfying when the capacity is over 250 mA h g^{-1} and plateau of potential above −0.850 V vs. Hg/HgO.

4. Conclusion

It is shown that the alloy of a composition $La_{0.8}Ce_{0.2}Ni_{2.5}Co_{1.8}Mn_{0.4}Al_{0.3}$, produced by mechanical alloying followed by annealing and activation, exhibits high specific capacity at the stable potential plateau, even at the high rate, and low hydrogen equilibrium pressure. The alloy of such composition gives low capacity lost during cycling, which enables its application for metal hydride battery production.

References

[1] J.J.G. Willems, K.H.J. Buschow, J. Less-Common Metals 129 (1987) 13.
[2] H.H. Van Mal, K.H.J. Buschow, F.A. Kuijpers, J. Less-Common Metals 32 (1973) 289.
[3] T. Sakai, K. Oguro, H. Miyamura, N. Kuriyama, A. Kato, H. Ishikawa, J. Less-Common Metals 161 (1990) 193.
[4] T. Sakai, H. Miyamura, N. Kuriyama, A. Kato, K. Oguro, H. Ishikawa, J. Less-Common Metals 159 (1990) 127.
[5] T. Sakai, H. Miyamura, N. Kuriyama, A. Kato, K. Oguro, H. Ishikawa, J. Electrochem. Soc. 137 (1990) 795.
[6] T. Saki, H. Yoshinaga, H. Miyamura, H. Ishikawa, J. Alloys and Comp. 180 (1992) 37.
[7] T. Sakai, T. Harama, H. Miyamura, N. Kuriyama, A. Kato, H. Ishikawa, J. Less-Common Metals 172–174 (1991) 1175.
[8] B.V. Ratnakumar, C. Witham, B. Fultz, G. Halpert, J. Electrochem. Soc. 141 (1994) 189.
[9] W. Zhang, A. Visintin, S. Srinivasan, A.J. Appleby, H.S. Lim, J. Power Sources 75 (1998) 84.
[10] M.P.S. Kumar, K. Petrov, W. Zhang, A.A. Rostami, S. Srinivasan, G. Adzic, J.R. Johnson, J.J. Reilly, H.S. Lim, J. Electrochem. Soc. 142 (1995) 3424.
[11] US Patent No. 5,605,585 (1997)
[12] A. Anani, A. Visintin, K. Petrov, S. Srinivasan, J. Power Sources 47 (1994) 261.
[13] C. Lenain, L. Aymard, F. Salver-Disma, J. Leriche, Y. Chabre, J. Tarascon, Solid State Ionics 104 (1997) 237.
[14] J.S. Benjamin, Sci. Am. 234/235 (1976) 40.
[15] C. Iwakura, Y. Kajiya, H. Yoneyama, T. Sakai, K. Oguro, H. Ishikawa, J. Electrochem. Soc. 136 (1989) 1351.